Journal of Thermal Analysis and Calorimetry, Vol. 72 (2003)1005–1017

DETERMINING THE MELTING BEHAVIOUR OF ASHES FROM INCINERATION PLANTS VIA THERMAL ANALYSIS

S. Arvelakis[*]*, F. J. Frandsen and K. Dam-Johansen*

CHEC Research Group, Department of Chemical Engineering, Technical University of Denmark, 20800 Lyngby, Denmark

Abstract

The ash behaviour comprises one major obstacle towards the efficient utilization of municipal solid wastes, (MSW), in incineration plants. The presence of large amounts of inorganic constituents such as alkali and alkali earth metals, chlorine, sulfur and zinc increase significantly the ash reactivity and lead to severe ash-related problems such as fouling, slagging, corrosion and erosion during their thermal treatment.

In this paper, the melting behaviour of various ash fractions originating from the incineration of MSW is studied using simultaneous, (DSC/TG), thermal analysis methods. The produced results provide the basis for improved modelling of the ash behaviour during the incineration of MSW.

Keywords: ash, corrosion, fouling, MSW, slagging, STA

Introduction

The amount of municipal solid wastes (MSW) is increasing dramatically worldwide, while their disposal has become an important global environmental and economical issue. Thermal disposal methods such as combustion and gasification can be an attractive solution regarding the safe and economical exploitation of MSW. In this way energy can be recovered, while the greenhouse gas emissions are reduced considerably and the amount of the final solid waste needed to be disposed and also the disposal area are also reduced significantly.[1–4]

MSW material much very diversified composition depending on the site of collection and contains a high amount of ash, the majority of which is present in very reactive forms including alkali and alkali earth metals as oxides, hydroxides, chlorides, sulfides and sulfates. Moreover, the amount of heavy metals such as zink, lead, copper, cadmium and arsenic appears also to be significantly higher than the trace level at which these elements normally are present in other materials such as coal and biomass, with zink to be present in concentrations corresponding to the main elements of the ash fraction.[5, 6] The presence of large amounts of the above mentioned inor-

* Author for correspondence: E-mail: sa@kt.dtu.dk

1388–6150/2003/ $ 20.00

Akadémiai Kiadó, Budapest
Kluwer Academic Publishers, Dordrecht

Table 1 Chemical composition of various ash samples using the ICP-OES analysis method

Samples	Alkalies	CaO	MgO	Fe_2O_3	P_2O_5	Al_2O_3	SiO_2
Bottom ash Untreated	4.1	35.44	3.78	5.53	1.88	17.28	20.66
Bottom ash Leached	5.09	27.96	3.6	7.8	2.09	14.13	30.44
Difference/%	24.14	21.10	–4.76	41.04	11.17	18.22	47.33
2–3rd pass ash Untreated	5.72	24.50	3.00	2.86	3.34	9.82	27.43
2–3rd pass ash Leached	2.30	26.46	3.33	3.14	3.80	10.96	28.93
Difference/%	–59.80	8.00	11.11	10.00	13.70	11.54	5.47
Superheater ash Untreated	15.96	16.52	2.00	2.00	2.75	5.48	15.21
Superheater ash Leached	2.13	24.78	3.17	3.14	4.17	8.31	24.00
Difference/%	–86.66	50.00	58.33	57.14	51.67	51.72	57.75
Economizer ash Untreated	15.90	16.94	2.17	2.00	2.89	6.23	15.43
Economizer ash Leached	2.04	24.08	2.83	3.14	4.58	9.26	24.21
Difference/%	–87.20	42.15	30.77	57.14	58.73	48.48	56.94
ESP ash Untreated	17.28	17.08	2.17	1.71	2.84	6.42	15.21
ESP ash Leached	2.21	23.24	3.17	3.00	4.49	10.39	24.64
Difference/%	–87.19	36.07	46.15	75.00	58.06	61.76	61.97

Table 1 Continued

Samples	TiO_2	CuO	PbO	ZnO	SO_3	Br	Cl
Bottom ash Untreated	2.51	0	0	1.1	5.63	0	1.39
Bottom ash Leached	4.66	0	0	1.57	2.32	0	0.23
Difference/%	85.65	0	0	42.72	58.792	0	–83.45
2–3rd pass ash Untreated	2.00	0.07	0.04	1.50	11.50	0.02	2.60
2–3rd pass ash Leached	2.17	0.09	0.05	1.74	10.75	<0.0025	0.06
difference/%	8.33	28.07	23.08	16.67	–6.52	–85.3	–97.88
Superheater ash Untreated	1.28	0.09	1.19	2.74	27.25	0.01	2.40
Superheater ash Leached	2.17	0.13	1.40	3.86	17.75	<0.0025	0.0015
Difference/%	68.83	42.86	18.18	40.91	–34.86	–77.27	–99.94
Economizer ash Untreated	1.37	0.19	0.94	5.48	21.25	0.07	6.40
Economizer ash Leached	2.00	0.34	1.19	8.22	14.75	<0.0025	0.0018
Difference/%	46.34	80.00	26.44	50.00	–30.59	–96.62	–99.97
ESP ash Untreated	1.35	0.28	1.00	5.98	12.00	0.23	16.10
ESP ash Leached	2.17	0.45	1.29	8.72	13.00	<0.0025	0.0047
Difference/%	60.49	63.64	29.03	45.83	8.33	–98.9	–99.97

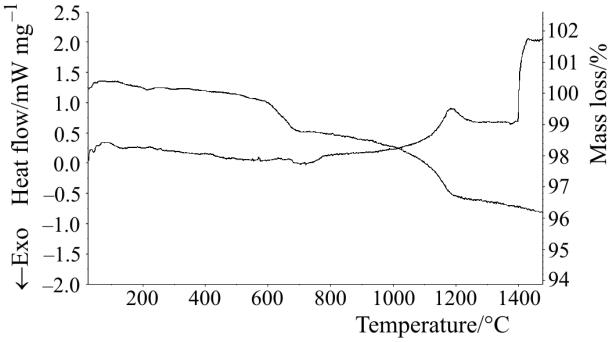

Fig. 1 Simultaneous thermal analysis of the bottom ash samples. Untreated bottom ash sample

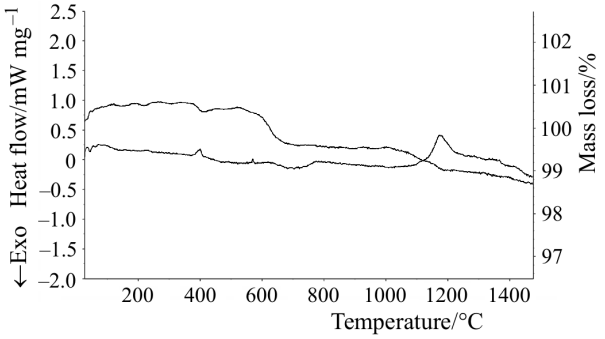

Fig. 2 Simultaneous thermal analysis of the bottom ash samples. Leached bottom ash sample

ganic constituents such as alkali and alkali earth metals, chlorine, sulphur and zink in very reactive forms e.g., chlorides, oxides, sulphates, increase significantly the ash reactivity of the MSW materials leading to severe ash problems such as fouling, slagging, corrosion and erosion during the thermochemical treatment [7, 8].

Thermal analysis methods (DTA, TG, DSC, TMA) alone or in combination with other analytical techniques such as FT-IR, SEM-EDX, XRD and mass spectrometry have been proved to be effective regarding the analysis and characterization of various materials such as coal, biomass, MSW and their mixtures [9–11, 18].

Several different characteristics of the above mentioned materials i.e. reaction rates, volatile content, calorific value, ash melting behaviour, etc., can be identified using thermal analysis methods [12–17, 19, 20]. In this paper the melting behaviour of five different ash fractions generated from the incineration of MSW material is studied using simultaneous (DSC/TG) thermal analysis.

Experimental

The material used in this study was ash from the Svendborg MSW incinerator situated in Svendborg, Denmark. In total five different ash fractions, collected from various parts of the incinerator, such as bottom ash, 2–3rd pass ash, superheater ash,

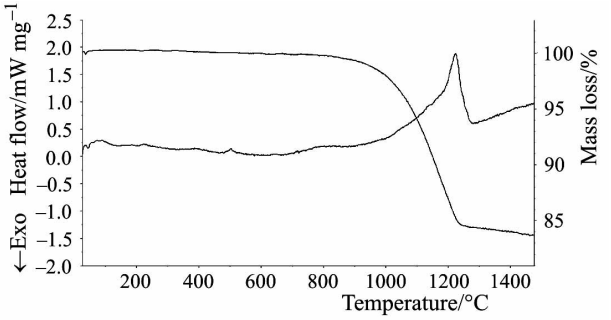

Fig. 3 Simultaneous thermal analysis of the 2–3rd pass ash samples. Untreated 2–3rd pass ash sample

economizer ash and ash from the electrostatic precipitator were studied. All the initial ash samples were leached using deionised water in order to remove the water-soluble salts condensed on the surface of the ash particles, in order to study their effect on the melting behaviour of the various ash fractions.

The leaching process, applied to each ash fraction, included the treatment of 250 g of ash material with one litre of deionised water under continuous steering at 70°C followed by filtration using a 0.045mm filter in a six-stage process. All the untreated and the leached ash samples were heated in a muffle furnace at 550°C in order to burn-off any carbon impurities present before studying their melting behaviour using the STA method.

The melting behaviour of the different ash samples before and after the leaching process was studied by using a simultaneous (STA) thermal analysis method. STA implies continuous measurement of sample mass (thermogravimetric analysis, TG) and temperature differential scanning calorimetry (DSC) during heat treatment. The mass measurement reveals any mass changes taking place in the sample and by comparing the sample temperature to the temperature of an inert reference material, any heat producing or heat consuming (chemical or physical) processes occurring in the sample is detected, and the involved energy subsequently quantified.

The experiments were carried out in a Netzsch STA 409°C, which was used in the differential scanning calorimetry/thermogravimetric analysis (DSC/TG) configuration.

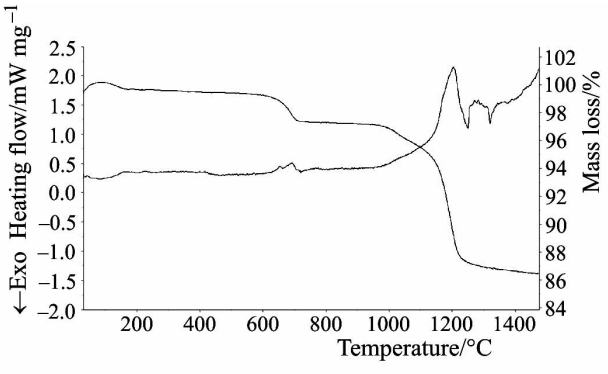

Fig. 4 Simultaneous thermal analysis of the 2–3rd pass ash samples. Leached 2–3rd pass ash sample

Table 2 Results from the STA runs using various ash fractions from MSW incineration

Sample	Final sample condition	Mass loss during various temperature segments/%		
		300–850°C	850–1150°C	1150–1450°C
Bottom ash untreated	Dark coloured glass deposite-white spots	1.5	1.38	1.00
Bottom ash leached	Dark coloured glass deposit-white spots	1.02	0.38	0.45
2–3rd pass ash untreated	Dark coloured glass deposit	0.60	8.90	6.90
2–3rd pass ash leached	Dark coloured glass deposit	2.33	2.96	7.80
Superheater ash untreated	Non glassy deposit+partially glassy deposit	0.90	10.98	13.94
Superheater ash leached	Half glass+half silicate-like deposit	0.33	11.48	10.63
Economizer ash untreated	Non glassy brown silicate deposit	1.11	14.06	15.92
Economizer ash leached	Dark coloured glass deposit	0.15	7.31	8.95
ESP ash untreated	Non glassy silicate deposit	2.20	30.40	12.26
ESP ash leached	Dark coloured glass deposit	0.53	9.72	7.77

The system was temperature and sensitivity calibrated with metal standards, at each heating rate in the applied temperature range, at each set of conditions. Platinum/rhodium crucibles with platinum lids were used. A thin alumina disc was placed beneath the crucibles in order to avoid platinum-platinum bonds between crucible and sample carrier. The ash samples were heated from 25 to 1470°C using a heating rate of 10°C min^{-1} in an inert atmosphere, using a nitrogen flow of 100mL min^{-1} as purge gas.

Results and discussion

Table 1 presents the elemental analysis of the various ash samples. The four fly ash samples (2–3rd pass, superheater, economizer and ESP) were analysed using the ICP-OES analysis method, while the bottom ash sample was analysed using the SEM-EDX analysis method due to the large in-homogeneity of this sample that makes the preparation of a quantitative representative analysis sample impossible. As it is seen from Table 1, the fly ash samples have a basic structure formed by silicon, calcium, alkali metals, aluminium, sulphur and chlorine in concentrations varying from 80–85 % depending on the sampling point downstream the reaction chamber. In addition, smaller amounts of other elements such as iron, magnesium, zink, titanium and phosphorus appear also to be present. Leaching appears to remove to a great ex-

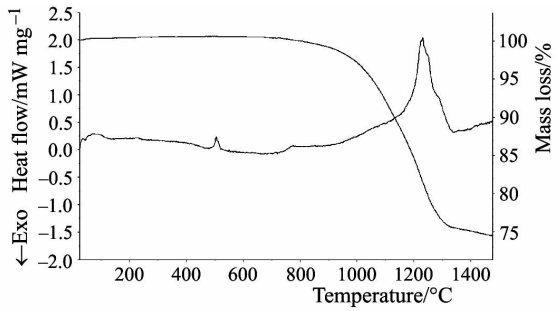

Fig. 5 Simultaneous thermal analysis of the Superheater ash samples. Untreated Superheater ash sample

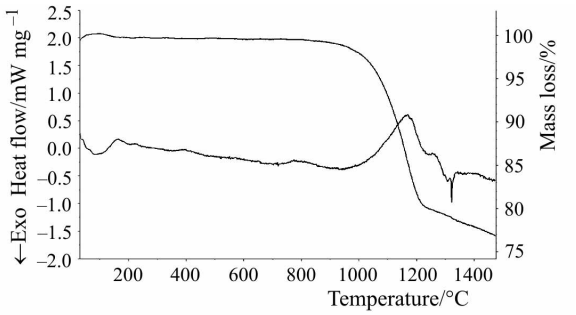

Fig. 6 Simultaneous thermal analysis of the Superheater ash samples. Leached Superheater ash sample

tent the alkali metals and chlorine, and in most of the cases partially the sulphur, showing that these elements are present in the ash material in the form of inorganic salt layers condensed heterogeneously on the surface of the residual ash particles. On the other hand, the concentrations of calcium, silicon, aluminium and also of elements such as zink, phosphorus, iron and magnesium appear to increase from 30–50 % accounting, in combination with sulphur, to almost 90 mass/mass% of the ash sample in all cases.

The SEM-EDX analysis of the bottom ash samples shows that the basic structure of the bottom ash is also formed from silicon, calcium and aluminium (>70 %), accompanied with smaller amounts of other elements such as alkali metals, sulphur, iron, phosphorus, chlorine etc. On the other hand, the large in-homogeneity of the specific ash fraction leads also to some controversial results such as an increase of the amount of alkali metals contained in the ash sample after the leaching process and a decrease of the amount of calcium and aluminium.

Bottom ash

Figures 1–2 and Table 2 present the results from the simultaneous thermal analysis of the initial and the leached bottom ash samples. As it is seen from Fig. 1, the DSC curve presents small endothermic peaks from 500–800°C accompanied by a minor mass loss of 1.5 % from 600–700°C, probably due to the dissociation of carbonates. At approximately 900°C the DSC curve starts to create a very distinct endothermic peak that is completed shortly after the 1200°C and is accompanied by a small mass loss of almost 1.2 %. The specific peak is attributed to the partial melting and evaporation of alkali and alkali earth metal chlorides, decomposition of alkali carbonates, and calcium sulphates and also to the melting of the potassium and calcium silicates forming the structure of the ash material. The visual inspection of the ash sample after the end of the STA process verifies these observations showing the formation of a glassy deposit according to the data depicted in Table 2.

On the other hand, leaching does not appear to improve significantly the thermal behaviour of the leached ash sample as it is seen in Fig. 2. The DSC curve shows again signs of endothermic processes taking place in the temperature range of

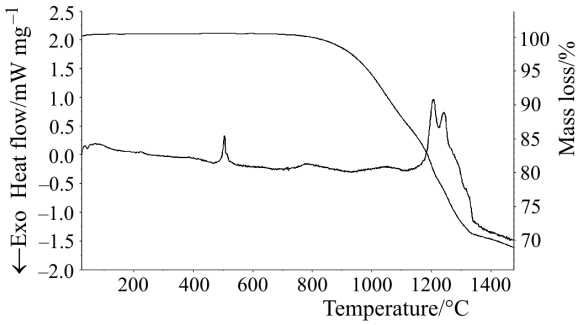

Fig. 7 Simultaneous thermal analysis of the Economizer ash samples. Untreated Economizer ash sample

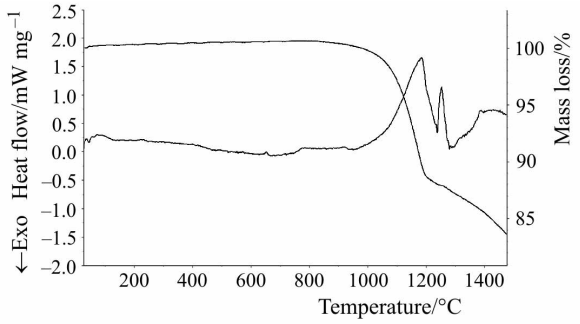

Fig. 8 Simultaneous thermal analysis of the Economizer ash samples. Leached Economizer ash sample

300–600°C, probably due to partially melting or dissociation of alkali and alkali earth metal hydroxides such as KOH and $Ca(OH)_2$, accompanied by a small mass loss of 1.2% as in the case of the untreated ash sample [7, 20]. A large endothermic peak appears again as in the case of the untreated ash sample starting at approximately 1000°C and ending at 1400°C that is attributed again to the melting interactions among the silicates and sulphates forming the structure of the ash sample and also to the partial decomposition of the melted alkali and calcium sulphates. The end product of the STA run appears to be again a glassy deposit as in the case of the untreated bottom ash sample verifying the melting phenomena taking place in the silicate structure of the sample during the thermal process.

2–3rd Pass ash

Figure 3 presents the results from the STA run with the untreated 2–3rd pass ash sample. The DSC curve shows the presence of only a minor endothermic peak in the temperature range of 300–750°C, probably due to the melting of alkali containing compounds such as sulphides [7]. In a second stage a not very distinct peak appears between 750 and 850°C and is followed by a large endothermic peak between 850 and 1300°C. A mass loss of almost 16 % accompanies the two subsequent DSC peaks. The observed mass loss is attributed to the melting and subsequent evaporation of alkali and possibly alkali earth metal chlorides, and to the decomposition of carbonates, and sulphates, which are expected to constitute a large fraction of the specific ash sample, see Table 1. Moreover, the final product of the STA run is according to Table 2 a dark coloured glassy deposit that indicates a melting of the aluminosilicate structure of the ash sample during the thermal treatment. The results from the STA run using the leached 2–3rd pass ash sample show that leaching appears to have controversial effects on the thermal behaviour of that specific ash sample. As it is seen from Fig. 4 two successive small endothermic peaks are identified between 600–700°C simultaneously with a mass loss of almost 2.3 %, most likely due to the decomposition of calcium carbonate. The main endothermic phenomena appear at higher temperature (950°C *vs.* 750°C) compared to the non-leached ash sample and

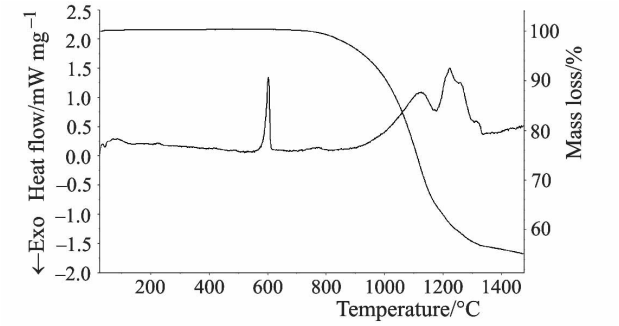

Fig. 9 Simultaneous thermal analysis of the ESP ash samples. Untreated ESP ash sample

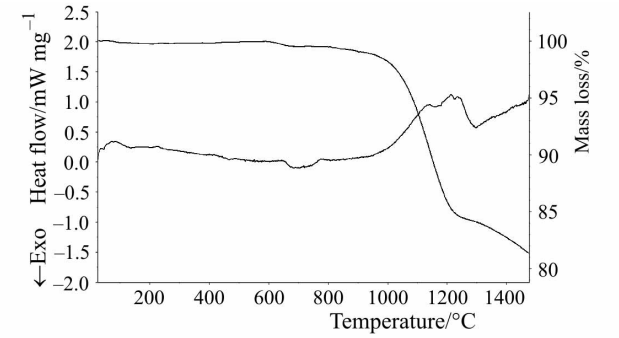

Fig. 10 Simultaneous thermal analysis of the ESP ash samples. Leached ESP ash sample

are accompanied by a lower mass loss, accounting for almost 10.5 % of the sample mass. This improved behaviour is attributed to the removal of alkali chlorides from the specific ash sample during the leaching process, see Table 1. However, the melting of the sample appears to end at a slightly higher temperature, compared to the case of the non-leached ash sample, showing that the removal of the alkali metals and chlorine does not affect the melting behaviour of the specific ash sample significantly. The inspection of the ash material after the end of the STA run shows the existence of a dark coloured glassy material as in the case of the non-leached ash sample.

Superheater ash

In Fig. 5 the thermal analysis of the non-leached superheater ash sample shows the presence of a small endothermic peak around 500°C probably due to the melting or transformation of an alkali-containing compound. The peak is not present in the DSC curve of the leached sample indicating that it most likely corresponds to a water-soluble compound. K_2SO_4 shows a phase transformation at approximately 600°C and thus the observed peak at 500°C might be due to this effect [11]. A large endothermic peak appears at the DSC curve a little above the temperature of 800°C, ac-

companied by a significant mass loss approaching 25 % of the sample mass. The mass loss observed is consistent with the results depicted in Table 1, showing a large amount of alkali and alkali earth metals, chlorine and sulphur present in the specific ash sample. The broad endothermic peak indicates also the initiation of a silicate melting process due to their interaction with the alkali and alkali earth metals. The inspection of the sample after the end of the STA test verifies this observation, showing that the ash material after the STA has been turned to a partially glassy, hard, material. The thermal treatment of the leached superheater ash sample shows no significant thermal effects until 900°C. Above this temperature, the DSC and TG curves show again the initiation of melting and evaporation/decomposition processes as in the case of the non-leached ash sample. Though the mass loss observed now, is slightly lower compared with the case of the non-leached ash sample, the melting phenomena addressed by the DSC peak show to end at a slightly lower temperature. The visual inspection of the heated ash sample, after the end of the process, shows again the formation of a partially glassy ash material. These results show that the presence of large amounts of alkali metals, chlorine and sulphur as water-soluble salts in the untrated ash sample does not affect the melting of the basic aluminosilicate structure of the ash negatively.

Economizer ash

Figure 7 presents the results from the STA run using the non-leached economizer ash sample. The chemical composition of this sample appears to be similar to that of the non-leached superheater ash sample according to Table 1 and so do the STA curves. Again, the DSC curve shows the existence of a small peak at 500°C without any mass loss due to the melting/transformation of alkali-containing compounds, with the phase transformation of K_2SO_4 appearing as the prevailing explanation [7, 11]. At higher temperatures a small not very distinct endothermic peak appears at the temperature range 700–800°C accompanied by a small mass loss of less than 1mass/mass% probably due to the decomposition of carbonates. As it is seen from the TG curve, a large mass loss accounting for almost 30 mass/mass% of the initial mass, starts at approximately 850°C and ends at 1450°C. This mass loss is accompanied by one small and not very distinct endothermic peak between 850–1100°C that is followed by two, large, overlapping peaks appearing from 1100 to 1350°C, attributed again to the melting and evaporation of alkali chlorides, to the decomposition of alkali and calcium sulphates and to the partial melting of silicates. The visual inspection of the ash material resulting from the STA process shows the presence of a hard brown silicate material. The material is not glassy probably due to the low amount of silicon and aluminium in its structure, which does not favour the vitrification of the ash material.
The STA results from the treatment of the leached economizer ash sample depicted in Fig. 8 reveal again an improved thermal behaviour for the first half of the STA run, compare to the non-leached ash sample. Both the DSC and the TG curves show no signs of reaction taking place until the temperature of 900°C approximately. At higher temperatures both curves show a combination of a large mass loss and two

large successive endothermic peaks. The observed mass loss is almost half of that observed during the test with the non-leached sample mainly due to extraction of chlorine and alkali metals from the ash sample during the leaching process. Inspection of the ash material after the end of the STA run shows formation of a glassy deposit due to the increased amounts of silicon and aluminium present in the ash material.

ESP ash

Figures 9–10 present the results from the thermal analysis of the ESP ash. An endothermic peak appears in the DSC curve at approximately 600°C corresponding to the phase transformation of K_2SO_4. The peak is not seen in the DSC curve of the leached sample, indicating that K_2SO_4 is extracted from the ash sample during the leaching process. Endothermic reactions appear to start around 700°C, in the case of the non-leached ash sample, with the DSC curve showing a small peak accompanied by a small mass loss of less than 1 % due to the decomposition of carbonates. A significant mass loss (>40 mass/mass%) in combination with two large and partially overlapping peaks appear in the temperature range of 800–1350°C due to the melting and evaporation of alkali chlorides, the decomposition of calcium sulphates and also melting of silicates. The visual inspection of the ash material after the end of the heat treatment, shows the formation of a non glassy silicate deposit due to the low amounts of silicon and aluminium in the initial ash sample.

In the case of the leached ash sample although a combination of the initiation of an endothermic process with a mass loss of almost 17 % is observed to start at approximately the same temperature level of 800°C as in the case of the non-leached ash sample, the observed phenomena show to conclude at a slightly lower temperature. The end product of the STA process is a dark coloured glassy material, see Table 2, indicating larger interaction among the aluminosilicate structure of the ash and the alkali and alkaline earth metals possibly due to closer contact after the removal of the inorganic salt layers from the surface of the ash particles during the leaching process.

Conclusions

Simultaneous thermal analysis appeared to provide valuable information regarding the thermal behaviour of the various ash fractions studied.

The endothermic phenomena described by the DSC curves appeared to terminate at higher temperatures in the case of the non-leached ash samples compared to the leached ash samples in most cases. The presence of large amounts of alkali metals, chlorine and partially sulphur as water soluble salt layers on the surface of the non-leached ash particles made difficult the accurate determination of the melting tendency of the ash aluminosilicate structure. Removal of these salt layers from the surface of the ash particles through the leaching process showed some evidence of increased melting tendency probably due to better physical contact and heat transfer among the ash particles. However, further studies are required for a solid interpreta-

tion of the produced STA results. The produced STA results will form the base for modeling the ash melting behaviour during the incineration of MSW.

References

1 X. Guo, Z. Wang, H. Li, H. Huang, C. Wu and Y. Chen, Energy and Fuels, 15 (2001) 1441.
2 C. Dong, B. Jin, Z. Zhong and J. Lan, Energy Conversion and Management, 43 (2002) 2189.
3 E. Ducarne, E. Marty, G. Martin and L. Delfosse, Fuel, 77 (1998) 1311.
4 L. Ruth, Prog. Energy Combust. Sci., 24 (1998) 545.
5 C. C. Wiles, Journal of Hazardous Materials, 47 (1996) 325.
6 S. V. Vassiliev, C. Danheux, Ph. Laurent, T. Thiemann and A. Fontana, Fuel, 78 (1999) 1131.
7 T. R. P. E. Miles, T. R. Miles Jr, L. L. Baxter, R. W. Bryers, B. M. Jenkins and L. L. Oden, Alkali deposits found in biomass power plants, Volumes I, II. NREL Subcontract TZ-2- 11226-1, 1995.
8 F. J. Frandsen, L. A. Hansen, H. S. Sørensen and K. Hjuler, Characterisation of ashes from biofuels, Final Report from EFP-95 Project, Journal No. 1323/95-0007, The Danish Energy Research Programme, 1998, ISBN 87-7782-000-2.
9 L. A. Hansen, F. J. Frandsen, K. Dam-Johansen, H. S. Sørensen and B-J. Skrifvars, Energy and Fuels, 13 (1999) 803.
10 M. Stenseng, A. Zolin, R. Cenni, F. Frandsen, A. Jensen and K. Dam-Johansen, J. Therm. Anal. Cal., 64 (2001) 1325.
11 L. A. Hansen, F. J. Frandsen, K. Dam-Johansen and S. Sørensen, Thermochim. Acta, 326 (1999) 105.
12 S. Arvelakis, C. Sotiriou, A. Moutsatsou and E. G. Koukios, J. Therm. Anal. Cal., 56 (1999) 1271.
13 E. Biagini, F. Lippi, L. Petarca and L. Tognotti, Fuel, 81 (2002) 1041.
14 M. Otero, C. Diez, L. F. Calvo, A. I. Garcia and A. Moran, Biomass and Bioenergy, 22 (2002) 319.
15 P. Wunsch, G. Matuschek and A. Kettrup, Thermochim. Acta, 263 (1995) 95.
16 Z. Sarbak and M. Kramer-Wachowiak, J. Therm. Anal. Cal., 64 (2001) 1277.
17 P. Ubbriaco, P. Bruno, A. Traini and D. Calabrese, J. Therm. Anal. Cal., 66 (2001) 293.
18 R. Bassilakis, R. M. Carangelo and M. A. Wojtowicz, Fuel, 80 (2001) 1765.
19 M. Remmler, F. D. Kopinke and U. Stottmeister, Thermochim. Acta, 263 (1995) 101.
20 Y. Xie, W. Xie, W.-P. Pan, A. Riga and K. Anderson, Thermochim. Acta, 324 (1998) 123.